Effect of Deposition, Sputtering, and Evaporation of Lithium Debris Buildup on EUV Optics

M.J. Neumann[1], M. Cruce[1], P. Brown[1], S.N. Srivasta[1], D.N. Ruzic[1], O. Khodykin[2]

[1]Department of Nuclear, Plasma, and Radiological Engineering, University of Illinois at Urbana, 103 S. Goodwin Avenue, Urbana, Illlinois, 61801

[2]Cymer, 17075 Thornmint Ct.San Diego, California, 92127

ABSTRACT

One of the critical issues within extreme ultraviolet (EUV) lithography is that of mirror lifetime and the degradation due to debris buildup from the EUV pinch. This work experimentally measures the mitigation of Li debris from collecting on the surface of EUV-like optics through combined use of a helium secondary plasma, evaporation from optic materials at elevated temperatures, and preferential sputtering off of the optic material. This leads to sputter enhanced removal of the lithium debris. This applied research expands the current knowledge base in understanding lithium interactions with a helium plasma and optic surfaces and provides a basis for analytical model development. The ultimate goal is to improve the current state of the art knowledge in lithium-optic material interactions, experimentally test mitigation and renewal of optic materials, and develop a relevant model for the predictive capabilities of the mirror optics while expanding the knowledge base of lithium transport and interaction. Experimental results are measured through the use of profilometry and AFM to quantify the ability to keep the EUV optic in an as received state while being exposed to EUV like lithium debris.

Keywords: EUVL, Debris, Lithium, Optics, Modeling, Secondary Plasma, Mirror Lifetime

INTRODUCTION

EUV mirror optics are subjected to degradation through four main pathways[1]. The first is buildup of low-energy neutral debris that is deposited on the surface of the mirror optic and acts to absorb and scatter EUV photons as the EUV photons are incident and when they are reflected by the underling mirror. The deposition of neutral flux on the surface of the optics leads to increased surface roughness which acts to scatter the incident EUV photons away from the desired focal point. A second pathway of mirror optic destruction comes from the sputtering of the optics by incident ions from the plasma pinch. The third pathway of optic destruction is the diffusion of debris material into the optic material which acts to change the mirror composition and change the indices of refraction. Debris generation can be limited to a certain extent, but this production cannot be eliminated in its entirety[2-4]. Optical mirror surfaces for lithium based EUV systems must be engineered to withstand a continuous bombarding flux of sub-keV lithium ions for a commercially-viable high volume manufacturing component.

Lastly, conventional EUV mirror optic materials can degrade rapidly at elevated temperatures of more than 200° C because of the enhanced thermal interdiffusion of the high and low index materials within the mirror structure, such as Si and Mo[5]. Lately, though, higher temperature mirror optics have been developed and tested. Various leading mitigation techniques to limit the amount of debris that ever reaches the collector optics include the use of mass-limited droplet targets, tape targets, ambient gas buffer, electrostatic repulsion fields, and permanent and pulsed magnetic fields, foil traps[6]. However, investigation into in situ mirror optics cleaning has been somewhat limited. High energy oxygen ions can mechanically break the molecular bonds of the surface molecules and remove them off of the surface. Atomic oxygen present in the plasma also readily reacts with the debris on the surface of the mirror optics and forms more volatile compounds which can be more easily evaporated or removed. However, these oxygen species are effective predominately on hydrocarbons and not condensable metal vapor debris. Oxygen species are also very reactive with the mirror optics itself, which will change the index of refraction and decrease

Emerging Lithographic Technologies XI, edited by Michael J. Lercel,
Proc. of SPIE Vol. 6517, 65172Y, (2007) · 0277-786X/07/$18
doi: 10.1117/12.711033

reflectivity. Also, oxygen only has a ~0.872 transmission coefficient. Figure 1 shows transmission coefficients of various gasses from 12-14 nm with a pressure of 10 mTorr.

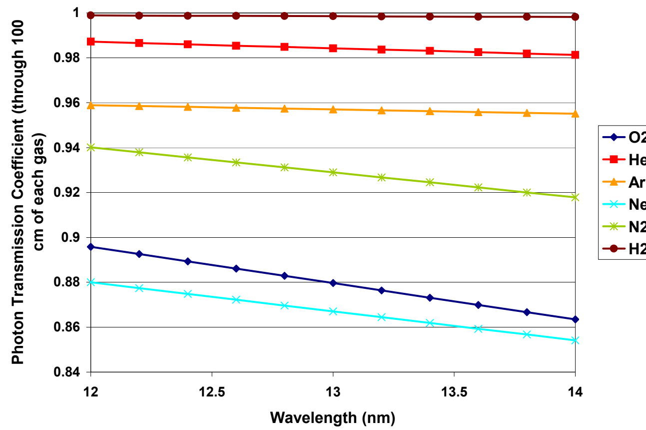

Figure 1. EUV photon transmission through 100 cm of various gases at 10 mT[7].

A helium plasma was chosen as the secondary plasma species because, as shown in figure 1, it has a high transmission coefficient of EUV photons and lithium compounds can be preferentially sputtered off the surface of mirror optics while the underlying mirror material has minimal damage. From modeling work with SRIM, various sputtering coefficients of He^+ at normal incidence on Li and mirror optic materials are shown in figure 6.

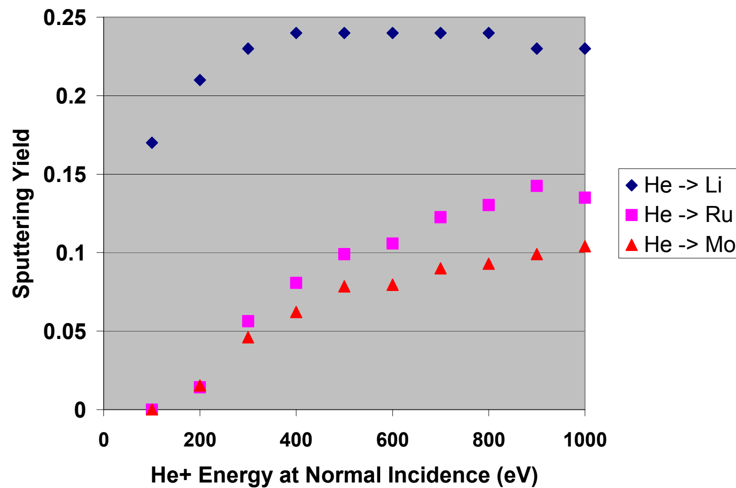

Figure 2. Selective sputtering coefficient of He+ on various materials[8].

From both the transmission and selective sputtering factors, helium was determined to be a good choice from the standpoint of EUV transmission.

Without in situ cleaning of the mirrors optics in an EUVL tool, Li debris will build up on the surface of the mirror optic and both absorb and scatter EUV photons away from the intermediate focus, thus decreasing efficiency, mirror lifetime, and contributing to a higher cost of ownership. The mirrors can be kept at an elevated temperature in situ to evaporated Li off of the surface, but not all Li compounds will evaporate because of their high binding energy to the surface and a debris film will accumulate that will absorb and scatter EUV photons. Also, care must be taken with the thermal load on the optics so as not to induce bilayer mixing.

An in situ secondary plasma, with high EUV photon transmission, can be used to selectively sputter off the Li debris without damage to the underlying mirror optic. However, again, a debris film will accumulate and act to absorb and scatter EUV photons. A secondary plasma in combination with elevated mirror temperature will lead to sputtering enhanced evaporation of Li debris from the mirror optic in situ during operation. This will minimize

debris buildup, preserve the stringent surface roughness requirements, extend mirror optic lifetime, and minimize tool downtime.

Because of these mirror lifetime issues and their critical importance, the brought about the need to simulate and study these anticipated device conditions while developing a model of all of the interactions occurring to as to improve the current state of the art knowledge in lithium-optic material interactions and expand the knowledge base of lithium transport and interaction. These driving factors led to the development of the *S*urface *C*leaning of *O*ptics by *P*lasma *E*xposure (SCOPE) experiment facility as described in the next section.

EXPERIMENT FACILITY

The SCOPE experiment facility is a multifunctional device that is capable of creating lithium debris conditions incident upon EUV optic materials so as to develop a model of lithium transport and operating regimes that will aid in the advancement of EUV mirror lifetime optics. SCOPE is composed of a unique sample holder, magnetron, and a secondary plasma source.

A 3" magnetron with a lithium target and a He plasma is used to sputter Li off of the target and deposit a Li film on mirror optic samples that is ~ 6 cm away. The sample holder is capable of providing DC and RF bias to a sample while at temperatures of up to 600° C and is fully rotatable to allow various incident angles between Li debris and the optic sample. Minimal out gassing occurs when the heater is in operation.

For the plasma cleaning portion of SCOPE, a helicon plasma source is employed at 13.56 MHz from 0-3 kW. The antenna used employed in SCOPE is an m = 0 helicon plasma stabilized with external magnetic fields. Helicon plasmas have been shown to have a good potential as a secondary plasma source in applications with no threat of contamination or further debris production[9].

The vacuum conditions and background composition of gas species present is monitored through the use of a residual gas analyzer. Contamination is minimized with the use of three halogen lights to bake out the system and a sample transfer system that is accomplished through the use of load lock with a magnetic transfer arm system.

While the description of the system may be straightforward, the integration of and use of these subsystems was not a trivial accomplishment and figures 3 provides and overview diagram of the SCOPE system to give one a picture of how this complex and multifunctional system comes together.

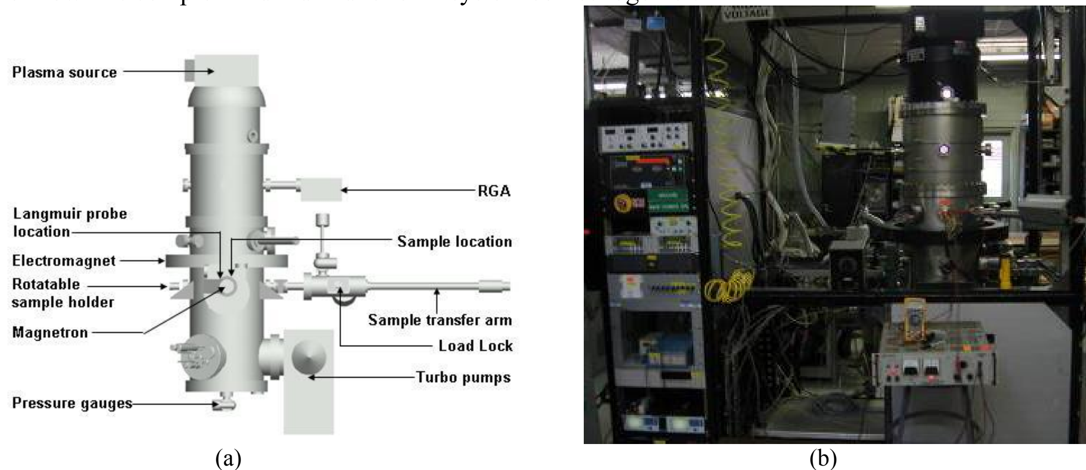

(a) (b)

Figure 3. (a) Schematic overview of the SCOPE facility. (b) Picture of SCOPE facility.

PLASMA CHARACTERIZATION

The first investigation to be undertaken was that of the plasma temperature and density. Using a RF compensated Langmuir probe, the temperature and density were measured over a 2-D region between the sample and the lithium magnetron for various conditions. The first condition was for a helium plasma at 20 mT and 65 W. The density and temperature profiles are shown in figure 4.

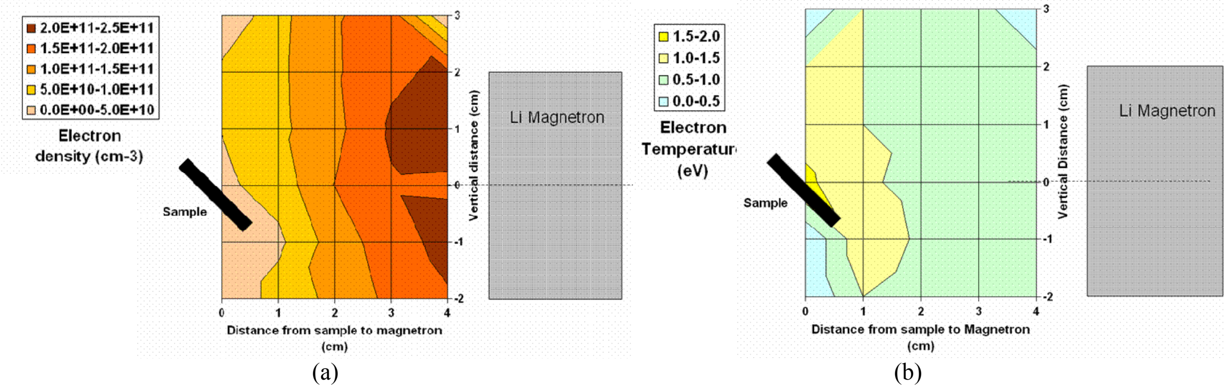

(a) (b)

Figure 4. (a) Electron temperature profile and (b) electron density profile for region between sample and magnetron for He plasma at 20 mT and 65 W.

The important point here is the electron temperature profile that is below 2 eV, which shows there is little to know sputtering of the resultant lithium debris on the sample after deposition because the energy of impinged particles is below the sputtering threshold. Next, the helium secondary plasma alone has a profile as shown in figure 5.

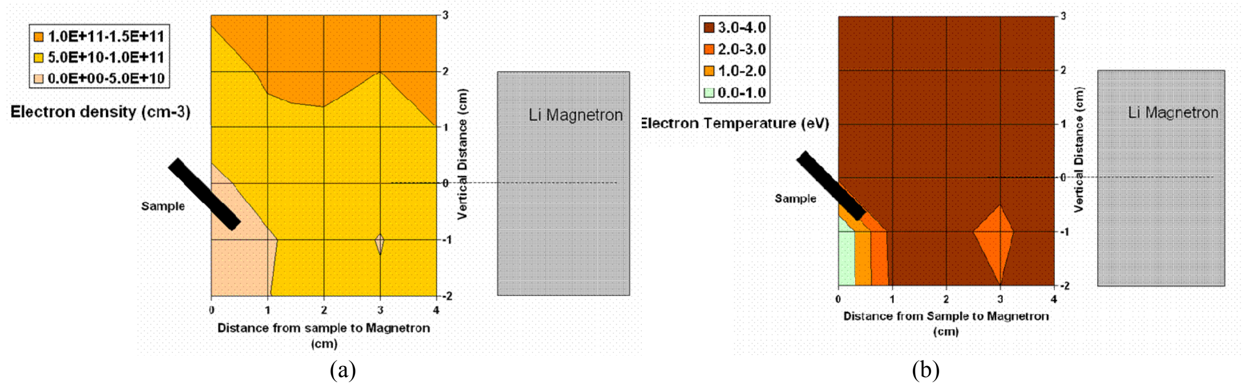

(a) (b)

Figure 5. (a) Electron temperature profile and (b) electron density profile for region between sample and magnetron with the helicon secondary He plasma at 20 mT and 3000 W.

Finally, a profile is constructed when both plasmas are on together and shown in figure 6..

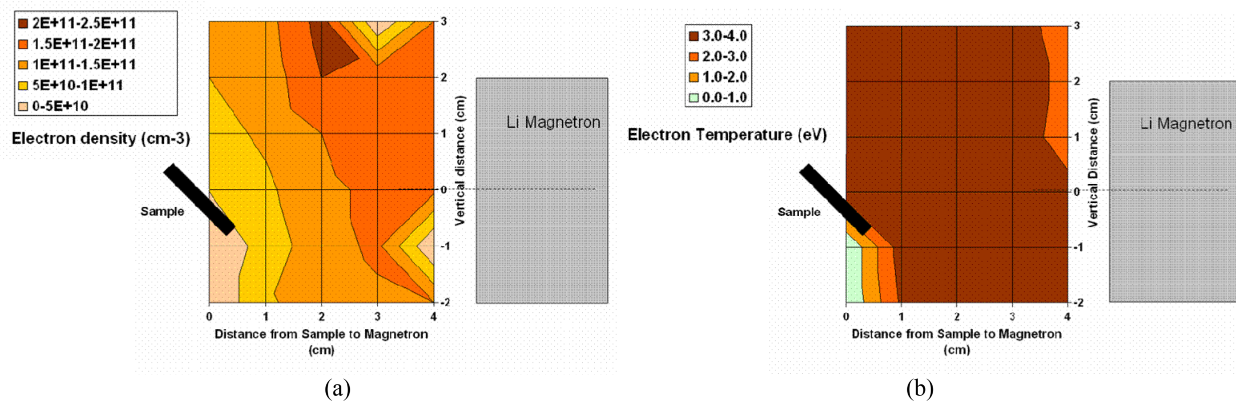

(a) (b)

Figure 6. (a) Electron temperature profile and (b) electron density profile for region between sample and magnetron with the helicon secondary He plasma and magnetron on at 20 mT and 3000 W.

This shows that with the presence of the secondary plasma, the density of He^+ ions around the sample is more than 10 times than with the magnetron density alone. Hence, there is increased mitigation between the magnetron and the sample and an increase He^+ flux to the sample. While the temperature is still below the sputtering threshold, with the application of a bias increase the sheath drop and the increased density, preferential sputtering of the lithium can be obtained, as shown in the next section.

PLASMA CLEANING RESULTS

The first step was to run a baseline lithium deposition protocol, to which all further plasma cleaning experiments would be compared. A helium plasma at 20 mT was struck on the lithium magnetron with a power of 65 W and was processed for 60 minutes. This resulted in a lithium film of 2250 $\pm$ 50 Å, as measured with profilometry and shown in figure 7.

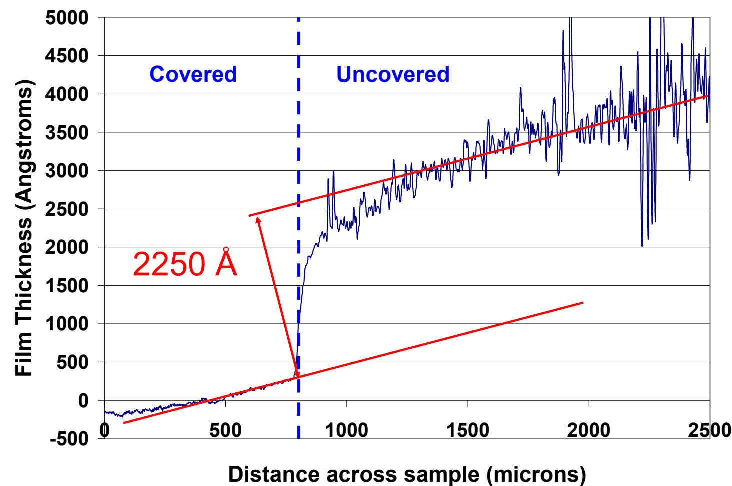

Figure 7. Resultant lithium film thickness after exposure to He magnetron plasma at 20 mT and 65 W for 60 minutes.

Subsequent AFM survey is shown in figure 8 and resulted in a surface roughness of 162 $\pm$ 5 nm.

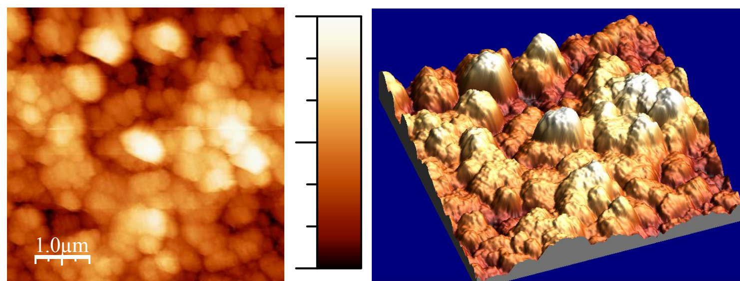

Figure 8. AFM analysis of resultant lithium film after exposure to He magnetron plasma at 20 mT and 65 W for 60 minutes.

This, clearly, would be a ruined EUV mirror and can be thought of as the worst case baseline scenario for this study. The film would aid in absorption of the EUV photons, while the surface roughness would act to scatter the EUV photons away from the desire focal point. Also, referencing the previous density as temperature measurements, the energy of the helium ions is such that there is little to no sputtering by the magnetron plasma itself.

The next step was to rerun the exact same deposition at the exact same conditions with the addition of thermal energy. The mirror was kept at 400° C throughout the deposition. Resultant film thickness measurement was 100 $\pm$ 2 Å, as shown in figure 9.

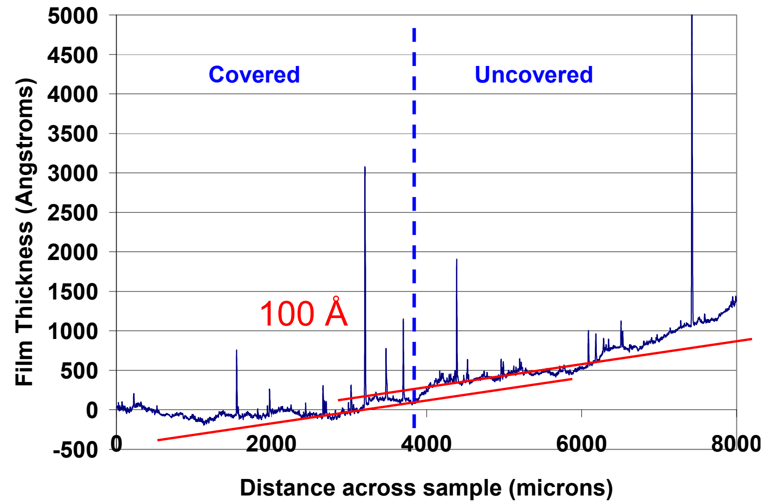

Figure 9. Resultant lithium film thickness after exposure to He magnetron plasma at 20 mT and 65 W for 60 minutes with the sample at 400° C.

While this shows a dramatic reduction in the resultant lithium debris film thickness, there is still a measurable and significant film present. This is confirmed through the correlating AFM analysis, as shown in figure 10.

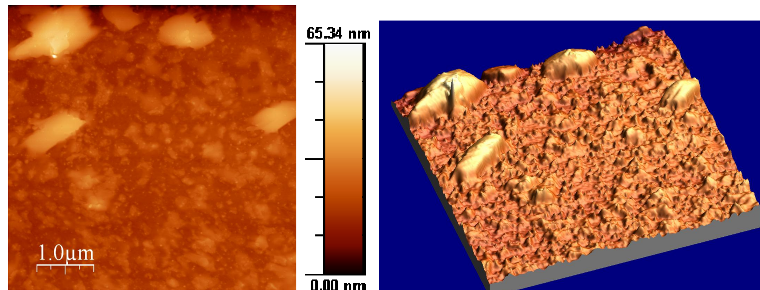

Figure 10. AFM analysis of resultant lithium film after exposure to He magnetron plasma at 20 mT and 65 W for 60 minute. with the sample at 400° C.

This surface roughness of 6 $\pm$ 1 nm is still enough to significantly scatter the impinging EUV photons, but it does show that heating aids in in situe mirror cleaning. Although, there is still significant debris left on the sample surface.

Moving on from here, the same lithium magnetron conditions were run on the next sample, but in addition, a 3000 W He plasma from a remote helicon antenna acting as a secondary plasma source was employed. The sample was kept at room temperature. The resultant lithium film of 900 $\pm$ 25 Å is shown in figure 11.

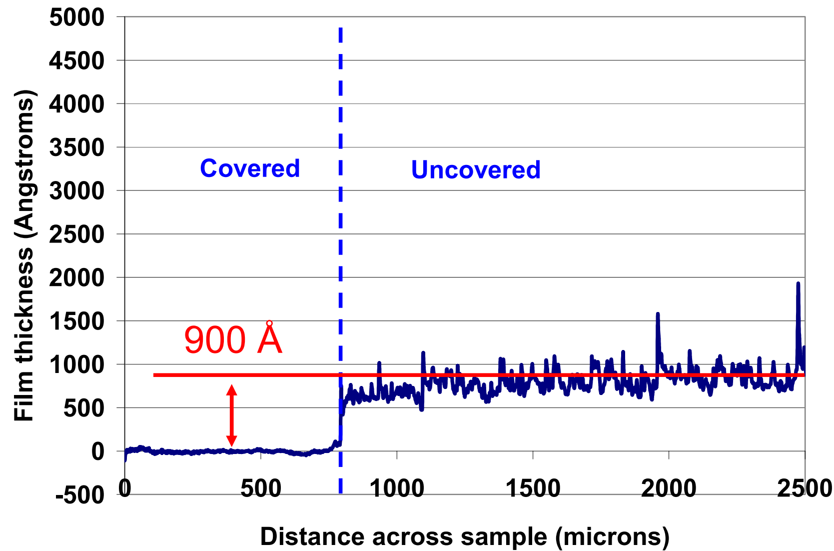

Figure 11. Resultant lithium film thickness after exposure to He magnetron plasma and secondary remote plasma at 20 mT and 65 W for 60 minutes with the sample at room temperature and 0 V bias.

This shows some improvement in resultant film thickness when compared to the baseline case, but it is not as effective in comparison to heating the sample. This is further confirmed through AFM analysis, which resulted in measure surface roughness of 215 ± 6 nm, as show in figure 12.

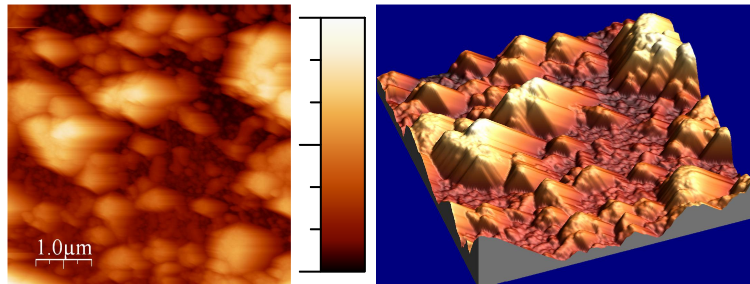

Figure 12. AFM analysis of resultant lithium film after exposure to He magnetron and secondary remote plasma at 20 mT and 65 W for 60 minutes with the sample at room temperature and 0 V bias.

This surface roughness, on first glance, looks worse than the baseline comparison case, but what should be noted is that the plasma is starting to break the lithium up such that the remaining debris is in clumps. This throws off the exactness of surface roughness measurements. While the energy of the impinging helium ions is below the sputtering threshold, there will be some ions in a Maxwellian distribution that have enough energy to sputter lithium. With the increased density of plasma due to the remote source, in comparison to the magnetron plasma alone, there is a net increase in those ions that do meet the sputtering threshold.

This result is much more dramatic when looking at the next experiment which was repeated in the same manner, but with -100 V bias, which accelerates the incident He^+ ions to at least 100 eV in potential, where there is a much greater sputtering yield. The resultant film thickness is on the order as without a bias, as shown in figure 13.

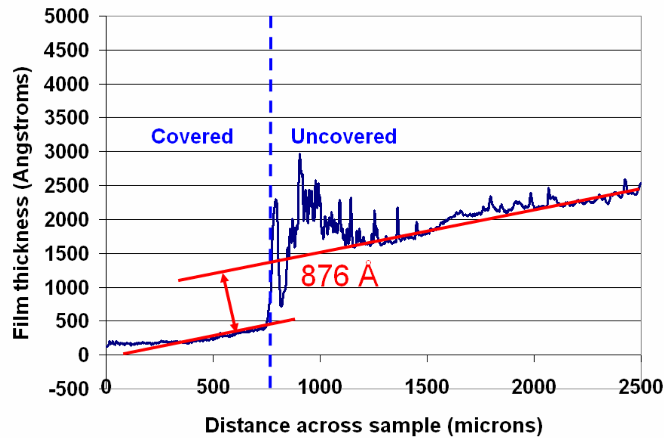

Figure 13. Resultant lithium film thickness after exposure to He magnetron plasma and secondary remote plasma at 20 mT and 65 W for 60 minutes with the sample at room temperature and -100 V bias.

This shows some decrease in film thickness compared to the grounded gase. However, the dramatic result is seen when looking at the AFM result in figure 14.

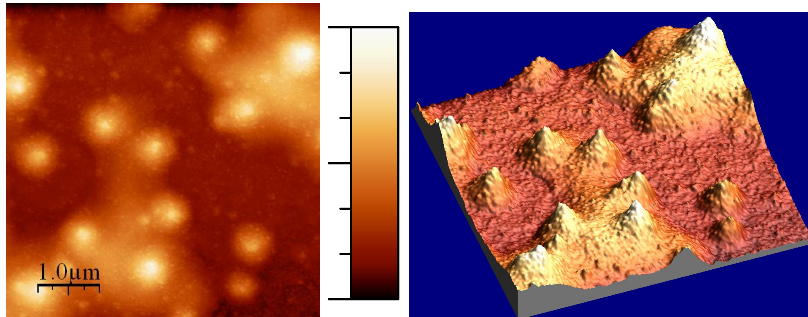

Figure 14. AFM analysis of resultant lithium film after exposure to He magnetron and secondary remote plasma at 20 mT and 65 W for 60 minutes with the sample at room temperature and -100 V bias.

Again, the surface roughness value of 52 $\pm$ 2 nm is not truly indicative of what the resultant surface is. When looking at the image created, it is seen that the lithium debris is in very discrete clumps. With the application of bias accelerating He^+ ions to above the sputtering threshold, there is a dramatic increase in sputtering of the lithium debris. Again, this is not as effective as heating alone, but the next experiment combined both techniques. The resultant film is negligible and shown in figure 15.

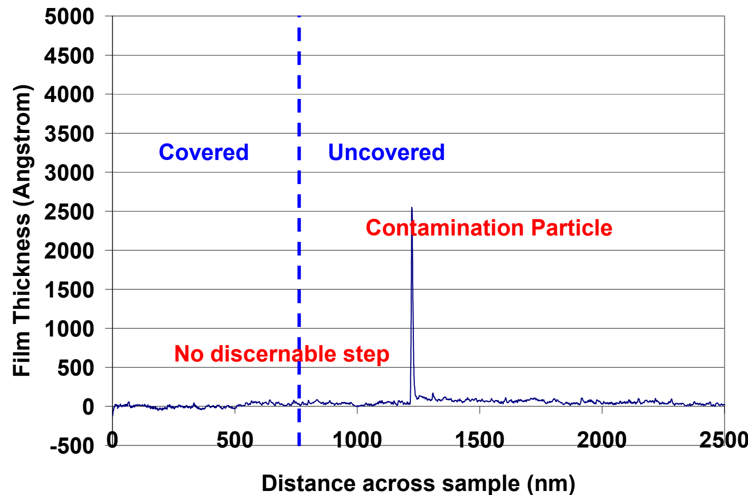

Figure 15. Resultant lithium film thickness after exposure to He magnetron plasma and secondary remote plasma at 20 mT and 65 W for 60 minutes with the sample at room temperature and -100 V bias.

The thickness of the film, if any, is below the resolution of the profilometer, which is less than 2 Å. The AFM survey, though, is the true proof of this successful concept and is shown in figure 16.

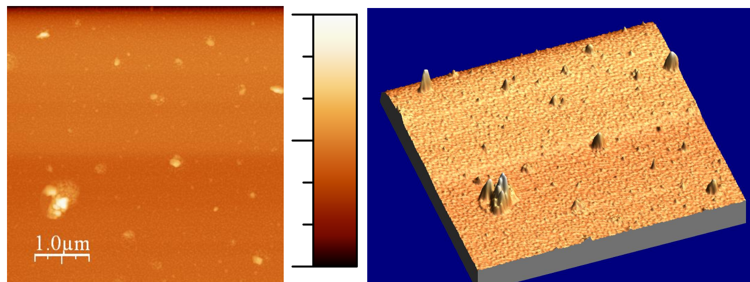

Figure 16. AFM analysis of resultant lithium film after exposure to He magnetron and secondary remote plasma at 20 mT and 65 W for 60 minutes with the sample at room temperature and -100 V bias.

The AFM analysis, which yielded a surface roughness of 4 $\pm$ 1 nm, but this is somewhat misleading. The surface roughness is actually much better, but is thrown off by the discrete clumps of resultant mirror debris. The combination of the increased plasma densit, bias acceleration, and heat leads to enhanced sputter evaporation of the lithium debris from the sample surface and leaves a much cleaner sample surface.

CONCLUSION

These experimental results clearly the benefit of an in situ secondary He plasma to aid in cleaning EUV optics during exposure to Li debris when heating alone cannot remove Li debris. The resultant sample surface is much smoother with much less debris present than those samples merely heated alone without the presence of the additional plasma. In situ secondary plasma cleaning can allow for longer lasting mirror optics at lower temperatures through sputtering enhanced evaporation. The next step is analytical model development and scaling to a commercial setting.

ACKNOWLEDGEMENTS

This work was supported by CYMER Inc under contract, Oleh Khodykin, Mgr., and INTEL Corporation under contract SRA 159-03, Robert Bristol Mgr. Special thanks to Alex Ershov, Oscar Hemberg, and Bill Marx at

CYMER Inc. Thanks to the Center for Microanalysis of Materials, which is supported by US DOE DEFG02-91-ER45439.

REFERENCES

[1] Ruzic, D.N., *Origin of Debris in EUV Sources and Its Mitigation*, in *EUV Sources for Lithography*, V. Bakshi, Editor. 2006, SPIE Press: Bellingham, Washington USA. p. 957-994.

[2] Stamm, U. and K. Gabel, *Technology for LPP Sources*, in *EUV Sources for Lithography*, V. Bakshi, Editor. 2006, SPIE Press: Bellingham, Washington USA.

[3]. Fomenkov, I.V., et al., *Dense Plasma Focus Source*, in *EUV Sources for Lithography*, V. Bakshi, Editor. 2006, SPIE Press: Bellingham, Washington USA. p. 373-393.

[4] Stamm, U., G. Schriever, and J. Kleinschmidt, *High-Power GDPP Z-Pinch EUV Source Technology*, in *EUV Sources for Lithography*, V. Bakshi, Editor. 2006, SPIE Press:

[5] Rettig, C.L., et al., *Protection of Collector Optics in an LPP Based EUV Source.* Emerging Lithographic Technologies IX, 2005. 5751: p. 910-918.

[6] Richardson, M., et al., *High conversion efficiency mass-limited Sn-based laser plasma source for extreme ultraviolet lithography.* Journal of Vacuum Science and Technology B: Microelectronics and Nanometer Structures, 2004. 22(2): p. 785-790.

[7] Henke, B.L., E.M. Gullikson, and J.C. Davis, *X-Ray Interactions: Photoabsorption, Scattering, Transmission, and Reflection at E=50-30,000 eV, Z=1-92.* Atomic Data and Nuclear Data Tables, 1993. 54(2): p. 181-342.

[8] SRIM, www.srim.org

[9] Hayden, D.B., et al., *Helicon plasma source for ionized physical vapor deposition.* Surface and Coatings Technology, 1999. 120-121: p. 401-404.